# Dark Radiation: Theory and Applications

Stephen Angus

based on

arXiv:1403:6473 (SA)

and

arXiv:1312.3947 (SA, Conlon, Marsh, Powell, Witkowski)

CTPU Journal Club
November 2014

# Outline

# Outline

# What is dark radiation?

- Dark radiation: hidden relativistic matter that contributes to the energy density of the universe.
- At CMB temperatures,

$$\rho_{\text{radiation}} = \rho_\gamma + \rho_\nu + \rho_{\text{hidden}} \,.$$

- Conventionally parametrised in terms of the "excess effective number of neutrino species", $\Delta N_{\text{eff}} = N_{\text{eff}} - 3.046$:

$$\rho_{\text{radiation}} = \rho_\gamma \left(1 + \frac{7}{8}\left(\frac{4}{11}\right)^{4/3} N_{\text{eff}}\right) \,.$$

NOTE: Not necessarily extra $\nu$s; $N_{\text{eff}}$ can be non-integer valued!

# Why dark radiation?

Experimental hints:

- Planck+WP+highL+BAO+$H_0$ results:
  $N_{\rm eff} = 3.52^{+0.48}_{-0.45}$,with $H_0 = 67.3 \pm 1.2\,\mathrm{km\,s^{-1}\,Mpc^{-1}}$.
  (arXiv:1303.5076, Planck Collaboration)
- One BBN-only study: $N_{\rm eff} = 3.50 \pm 0.20$ (arXiv:1308.3240).
- [BICEP2: $r > 0$. Having more DR can reduce tension with Planck.
  $N_{\rm eff}^{(r=0.2)} = 4.00 \pm 0.41$ (Planck+WP+BICEP2) (arXiv:1403.4852).]

Can we trust these values?

- Results may favour a small DR contribution.
- Need to wait until the dust settles!

# Why dark radiation?

**Disclaimer**

In this talk: axion $\equiv$ axion-like particle (ALP).

String theory perspective:

- Generically $\mathcal{O}(100)$ gravitationally-coupled moduli (scalars), each with associated axions, many of which can remain massless.
- After inflation, universe reheated by decays of the lightest moduli.
- Any non-zero branching ratio to light hidden states is a source of dark radiation!

General considerations:

- Simple and natural extension of $\Lambda$CDM — if DM, why not DR?
- No a-priori reason why $N_{\text{eff}} = 3.046$ (eg. not symmetry-protected).

Harder to argue why dark radiation should *not* exist!
(Conversely, if $N_{\text{eff}} = 3.046$, string theory models must explain why.)

# Reheating

What happens after inflation?

- Any gravitationally-coupled scalar particles (eg. moduli in string theory) have generically acquired large non-zero VEVs.
- Begin to oscillate coherently about their final vacuum.
- Redshift as matter, $\rho_M \sim a^{-3}$; any radiation redshifts as $\rho_R \sim a^{-4}$.
- Moduli come to dominate the energy density of the universe; reheating is driven by the last modulus to decay.
- Final modulus $\Phi$ decays into visible and hidden-sector particles, with comparable decay rates,

$$\Gamma \sim \frac{m_\Phi^3}{M_P^2}\,.$$

Take-home message: the *lightest* modulus is *last* to decay.

# Cosmic Axion Background

- Decay to axions can occur via an interaction Lagrangian

$$\mathcal{L} \supset \frac{2}{\sqrt{6}M_P} \Phi \partial_\mu a \partial^\mu a \,.$$

- This produces pairs of axions, each with energies $E_a = m_\Phi/2$.
- These axions are highly relativistic and stream freely.

- Present day: would form a Cosmic Axion Background 1305.3603 (Conlon, Marsh).
- Can test CAB hypothesis via:
  - CMB, $N_{\rm eff}$;
  - axion-photon conversion in galaxy cluster B-fields;
  - 3.5 keV line: DM $\to a \to \gamma$ in clusters/galaxies.

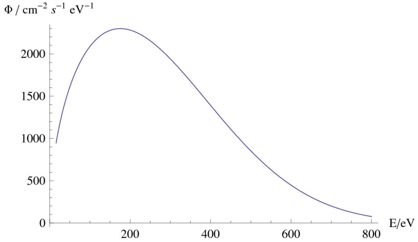


**Figure:** CAB, for $N_{\rm eff} = 3.62$.

# Outline

# LARGE Volume Scenario — overview

- Compactification of type IIB string theory where the Calabi-Yau volume $\mathcal{V}$ is stabilized to be exponentially large.
- Field content always includes:
  - the volume modulus, $\Phi$, whose large VEV fixes the volume;
  - its axion partner, the volume axion $a_b$.
- Realise (MS)SM on D3 branes at a singularity $\Rightarrow$ sequestering of soft masses:

$$M_{\text{soft}} \sim m_0 \sim m_{1/2} \sim \frac{M_{\text{P}}}{\mathcal{V}^2} \, .$$

Some reasons to have a sequestered visible sector:

- makes $\Phi \to$ visible kinematically viable;
- avoids Cosmological Moduli Problem (light moduli spoil BBN) for TeV-scale soft terms $\Rightarrow m_\Phi \sim 5 \times 10^6$ GeV.

Alternatively: D7s on fibre cycle (Hebecker *et al*, arXiv:1403.6810).

# LARGE Volume Scenario — mass hierarchy

**Hierarchy of scales:**

$$\begin{aligned} M_{\text{string}} &\sim \frac{M_{\text{P}}}{\mathcal{V}^{1/2}} \\ m_{\Phi} &\sim \frac{M_{\text{P}}}{\mathcal{V}^{3/2}} \\ M_{\text{soft}} &\sim \frac{M_{\text{P}}}{\mathcal{V}^{2}} \\ m_{a_b} &\lesssim M_{\text{P}}\, e^{-2\pi\mathcal{V}^{2/3}} \sim 0\,. \end{aligned}$$

- Note that the volume axion $a_b$ is effectively massless $\Rightarrow$ candidate for dark radiation.
- The leading decay modes of $\Phi$ are:
  - $\Phi \rightarrow a_b a_b$ (hidden);
  - $\Phi \rightarrow H_{\text{u}} H_{\text{d}}$ (visible).
- Other hidden sector channels possible (won't discuss here).
- Shift symmetry in Higgs sector $\Rightarrow Z = 1$ at the string scale.

Interaction Lagrangian:

$$\mathcal{L} \supset \frac{2}{\sqrt{6}M_{\text{P}}}(\partial_\mu a_b)^2\,\Phi + \frac{1}{\sqrt{6}M_{\text{P}}}\left[Z\,H_{\text{u}}H_{\text{d}}\,\Box\Phi + \text{h.c.}\right].$$

# Results for the one-axion model

- Minimal LVS: MSSM spectrum; Giudice-Masiero coupling $Z = 1$.
- Tree-level result: $\Delta N_{\text{eff}} \simeq 1.7$, in conflict with observation
  arXiv:1208.3562 (Cicoli, Conlon, Quevedo),
  1208.3563 (Higaki, Takahashi).
- Include loop corrections $\Rightarrow$ lower bound of

$$\Delta N_{\text{eff}} \gtrsim 1.4 \,,$$

  which is not much better than the tree-level result!
  arXiv:1305.4128 (SA, Conlon, Haisch, Powell)
- Exhibits the "moduli-induced axion problem": too much DR
  arXiv:1304.7987 (Higaki, Nakayama, Takahashi).

# Fibred scenario: two axions

- The minimal scenario appears to be ruled out!
- Need to look for alternative scenarios...
- Simple extension: fibred LVS compactifications (e.g. K3 or $T^4$ fibrations over a $\mathbb{P}^1$ base).
- Now two bulk moduli, each with associated axions.
- Visible sector on D3 branes at a singularity $\Rightarrow$ sequestering.
- Bulk volume takes the form $\mathcal{V} \simeq \sqrt{\tau_1}\tau_2$ .

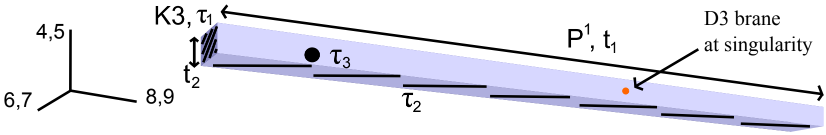


- $\tau_3$: small local cycle wrapped by ED3s; gives LARGE volume $\mathcal{V}$.

# Fibred LVS — mass hierarchy

**New hierarchy of states:**

$$
\begin{aligned}
M_{\text{string}} &\sim \frac{M_P}{\mathcal{V}^{1/2}} \\
m_{\Phi_{\mathcal{V}}} &\sim \frac{M_P}{\mathcal{V}^{3/2}} \\
m_{\Phi_{\Omega}} &\sim \frac{M_P}{\mathcal{V}^{3/2}\tau_1^{1/4}} \\
M_{\text{soft}} &\sim \frac{M_P}{\mathcal{V}^{2}} \\
m_{a_1,a_2} &\lesssim M_P\, e^{-2\pi\mathcal{V}^{2/3}} \sim 0\,.
\end{aligned}
$$

- One linear combination of moduli corresponds to the large bulk volume $\mathcal{V} \simeq \sqrt{\tau_1}\tau_2$.
- Flat transverse direction $\Omega$, lifted by string loop corrections (from D7 branes on $\tau_1$ and $\tau_2$) $\Rightarrow$ transverse combination $\Phi_\Omega$ is now the lightest modulus!
- Predictions of this scenario different from minimal LVS.
- Assume $\tau_1/\tau_2 \sim 10^{\pm\,\text{only a few}}$ $\Rightarrow$ ensures $m_{\Phi_{\mathcal{V}}} \gg m_{\Phi_\Omega}$.

# Decay to axions

- Kähler potential for bulk moduli & axions ($T_i \equiv \tau_i + i a_i$):

$$K = -2\ln\mathcal{V} \sim -\ln(T_1 + \bar{T}_1) - 2\ln(T_2 + \bar{T}_2)\,.$$

- Normalise $\Phi_1 = \frac{1}{\sqrt{2}}\ln\tau_1$, $\Phi_2 = \ln\tau_2$; rotate to mass eigenbasis (Burgess *et al*, arXiv:1005.4840)

$$\Phi_{\mathcal{V}} \equiv \sqrt{\frac{2}{3}}\Phi_2 + \sqrt{\frac{1}{3}}\Phi_1\,, \qquad \Phi_\Omega \equiv \sqrt{\frac{1}{3}}\Phi_2 - \sqrt{\frac{2}{3}}\Phi_1\,.$$

- Kinetic terms give interaction Lagrangian

$$\mathcal{L}_{\Phi_\Omega\to aa} = \frac{1}{\sqrt{3}M_\mathrm{P}}\Phi_\Omega\left(2\partial_\mu a_1\partial^\mu a_1 - \partial_\mu a_2\partial^\mu a_2\right)\,.$$

**Resulting decay rate to axions:**

$$\Gamma_{\Phi_\Omega\to aa} = \frac{5}{96\pi}\frac{m^3_{\Phi_\Omega}}{M^2_\mathrm{P}}\,.$$

# Decays to visible matter

- Decay to Higgs bosons: Kähler potential for vector-like matter is

$$K = -2\ln\mathcal{V} + \left\{ \frac{H_u \bar{H}_u + H_d \bar{H}_d + (Z H_u H_d + \text{h.c.})}{\left(T_1 + \bar{T}_1\right)^{1/3}\left(T_2 + \bar{T}_2\right)^{2/3}} \right\} .$$

- Relevant terms in the Lagrangian are

$$\mathcal{L} \supset -\frac{1}{\sqrt{6}M_P}\Phi_{\mathcal{V}}\left[H_u \Box \bar{H}_u + H_d \Box \bar{H}_d + \text{h.c.}\right] - \frac{1}{\sqrt{6}M_P}\left[Z H_u H_d \Box \Phi_{\mathcal{V}} + \text{h.c.}\right] .$$

  - 1st line: present for all matter scalars.
  - 2nd line: present for only vector-like matter.
- No longer any tree-level coupling to $\Phi_\Omega$!

# Decays to visible matter

Other visible sector decays:

- matter scalars — similarly no tree-level coupling to $\Phi_\Omega$;
- fermions — interactions chirality-suppressed, decays at loop level;
- gauge bosons — axions in the bulk, SM localised
  $\Rightarrow$ coupling $\mathcal{V}$-suppressed, also appears at loop level;
- other vector-like states — same story as for the Higgs bosons.

**Conclusion:**

NO tree-level decays of lightest modulus $\Phi_\Omega$ to visible matter!

# Consequences for $\Delta N_{\text{eff}}$

- Amount of dark radiation fixed by the ratio of branching ratios,

$$\kappa \equiv \frac{\mathrm{Br}(\text{hidden})}{\mathrm{Br}(\text{visible})} = \frac{\mathrm{Br}(\Phi_\Omega \to aa)}{\mathrm{Br}(\Phi_\Omega \to \text{visible})} .$$

- Estimate decay rate to visible sector:

$$\Gamma_{1-\mathrm{loop}} \sim \frac{1}{16\pi}\left(\frac{\alpha_{\mathrm{SM}}}{4\pi}\right)^2 \frac{m^3_{\Phi_\Omega}}{M_P^2} ,$$

so

$$\kappa \equiv \frac{\mathrm{Br}(\text{hidden})}{\mathrm{Br}(\text{visible})} \sim \frac{5}{6}\left(\frac{4\pi}{\alpha_{\mathrm{SM}}}\right)^2 \sim 10^4 .$$

**Result:**

$\Delta N_{\text{eff}} \gtrsim 3\kappa$, so $\Delta N_{\text{eff}} \gtrsim 3 \times 10^4 \Rightarrow$ completely excluded!

# Alternative scenario

Alternatively:

- Visible sector on D7s wrapping the fibre cycle $\tau_1$
  arXiv:1403.6810 (Hebecker, Mangat, Rompineve, Witkowski).
- Gauge kinetic function $f_{\text{vis}} = T_1 + hS$, $\text{Re}(f) \sim 1/g_{\text{SM}}^2$,
  for $g_{\text{SM}} \sim \mathcal{O}(1)$ consider limit where $\tau_2 \gg \tau_1$ ("anisotropic limit").
- Decay to Higgs restored; also decay to gauge bosons,

$$\Gamma = \frac{N_g}{48\pi} \gamma^2 \frac{m_{\Phi_\Omega}^3}{M_P^2} \quad , \quad \gamma = \frac{\tau_1}{\tau_1 + h\text{Re}(S)} .$$

- With $Z = 1$ and $\gamma = 1$ find a dark radiation abundance

$$\Delta N_{\text{eff}} \simeq 0.6 .$$

- Natural parameter values allowed by data!

# Summary I

- Dark radiation is a well-motivated addition to $\Lambda$CDM.
- The LARGE Volume Scenario in IIB String Theory is a good framework for building and testing models of the early universe.
- Constraints on $N_{\rm eff}$ provide a powerful test of such models.
- Minimal LVS is in tension with Planck data, so need to look at more complicated scenarios; fibred models qualitatively different.
- Fibred sequestered scenario: $\Delta N_{\rm eff} \gtrsim 3 \times 10^4$ (c.f. $\Delta N_{\rm eff} \simeq 0.5$) $\Rightarrow$ fibred sequestered models ruled out.
- D7s on the fibre cycle $\Rightarrow$ $\Delta N_{\rm eff} \simeq 0.6$, consistent with data.

However…

- If BICEP2 were to be confirmed, $\Delta N_{\rm eff} \simeq 1.0 \pm 0.4$ at 68% c.l. $\Rightarrow$ consistent with minimal LVS, where $\Delta N_{\rm eff} \gtrsim 1.4$.
- Watch this parameter space!

# Outline

# A brief history of the soft X-ray excess

- First discovered in 1996 by Extreme Ultraviolet Explorer (EUVE).
- Excess of low-energy (soft) X-rays detected at $\sim 138\,\mathrm{keV}$ in Virgo and Coma clusters.
- Consolidated by the ROSAT all-sky survey (1990 – 1999).
- ROSAT used position-sensitive proportional counters (PSPCs) with low internal backgrounds to scan energies $0.1 - 2.4\,\mathrm{keV}$. Low resolution but large field of view: ideal for diffuse emission.
- Bonamente et al. (2002) used ROSAT data to study 38 clusters — found that soft excess X-ray emission is a generic feature.
- Next-generation experiments XMM-Newton, Chandra and Suzaku also studied the soft excess, but have small fields of view — suboptimal, as background subtraction is harder.

# Soft X-ray excess from EUVE/ROSAT

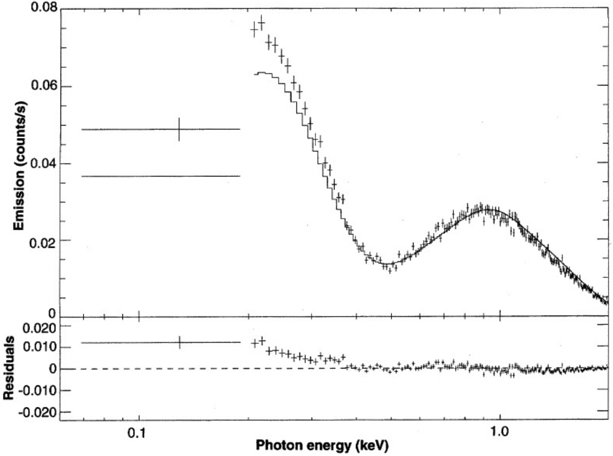


**Fig. 2.** Performance of the best fit MEKA single-temperature model (solid line) in a simultaneous fit to the EUVE DS and ROSAT PSPC data (the former is the first data point). The count rates correspond to those of the detected emission, and the residual is the difference between measured and model count rates.

# Properties of the soft X-ray excess

Features of the soft excess:

- It is soft: predominantly seen in ROSAT R2 band ($E \lesssim 0.38\,\mathrm{keV}$).
- Present for both nearby and distant clusters ($z \sim 0.3$), but only observed for clusters away from the galactic plane, where $N_{\mathrm{H}} \lesssim 5 \times 10^{20}\,\mathrm{cm}^{-2}$.
- Preferentially found away from the cluster centre, at $r \gtrsim 150\,\mathrm{kpc}$.
- Extends far beyond the cluster core, up to $r \lesssim 5\,\mathrm{Mpc}$ (cluster size is typically $\sim 1\,\mathrm{Mpc}$).
- Background: thermal bremmstrahlung, weakest (at low energies) for high-temperature, low density clusters, e.g. Coma.

# Axion-photon conversion

- Axions mix with photons via the term

$$\mathcal{L} \supset \frac{1}{4M} a F_{\mu\nu} \tilde{F}^{\mu\nu} \equiv \frac{1}{M} a \vec{E} \cdot \vec{B} \,.$$

- In the presence of a magnetic field, axions convert into photons (in a process analogous to neutrino oscillations).
- Typically this interaction is very weak, but can produce an observable effect over the scale of a galaxy cluster (eg. Coma).
- Linearised wave equation for the coupled axion-photon system:

$$\left( \omega + \begin{pmatrix} \Delta_\gamma & 0 & \Delta_{\gamma ax} \\ 0 & \Delta_\gamma & \Delta_{\gamma ay} \\ \Delta_{\gamma ax} & \Delta_{\gamma ay} & \Delta_a \end{pmatrix} - i\partial_z \right) \begin{pmatrix} |\gamma_\perp\rangle \\ |\gamma_\parallel\rangle \\ |a\rangle \end{pmatrix} = 0 \,,$$

where $\Delta_\gamma = -{\omega_{\rm pl}}^2/2\omega$, $\Delta_{\gamma ai} = B_i/2M$ and $\Delta_a = -{m_a}^2/\omega$.

# Propagation over a single coherent domain

- Conversion probability for propagation through a homogeneous magnetic field in a domain of size $L$:

$$P(a \to \gamma) = \sin^2(2\theta) \sin^2 \left( \frac{\Delta}{\cos 2\theta} \right) ,$$

where $\tan 2\theta = \frac{2B_\perp \omega}{M m_{eff}^2}$, $\Delta = \frac{m_{eff}^2 L}{4\omega}$ and $m_{eff}^2 = {m_a}^2 - {\omega_{pl}}^2$.

- Definitions:
  - $\omega$ is the axion energy (also the energy of the converted X-ray);
  - $\omega_{\mathrm{pl}}$ is the plasma frequency of the ICM, $\omega_{pl} = \sqrt{\frac{4\pi\alpha n_e}{m_e}} \sim \sqrt{n_e}$;
  - $B_\perp$ is the magnetic field component transverse to propagation;
  - $M$ is the inverse axion-photon coupling;
  - $m_a$ is the axion mass.

# Propagation over a single coherent domain

- Conversion probability for propagation through a homogeneous magnetic field in a domain of size $L$:

$$P(a \to \gamma) = \sin^2(2\theta)\sin^2\left(\frac{\Delta}{\cos 2\theta}\right) ,$$

where $\tan 2\theta = \frac{2B_\perp \omega}{M m_{eff}^2}$, $\Delta = \frac{m_{eff}^2 L}{4\omega}$ and $m_{eff}^2 = m_a{}^2 - \omega_{pl}{}^2$.

- Interesting physics requires $\omega_{\rm pl} \gtrsim m_a$; for simplicity we set $m_a = 0$.
- For the Coma cluster, $\theta \sim 10^{-5}$ so the small-$\theta$ approximation is always valid, giving $P(a \to \gamma) \simeq \theta^2 \sin^2(\Delta)$, with $\theta \simeq \frac{B_\perp \omega}{M \omega_{\rm pl}{}^2}$.
- Hence even averaged over many domains, $\langle P(a \to \gamma)\rangle \sim M^{-2}$.
- We will make use of this fact later!

# Coma magnetic field model

- In order to simulate axion-photon conversion in the Coma cluster, need to construct a plausible magnetic field model.
- We simulate the magnetic field in Coma using a stochastic model (Murgia et al., 2004) that fits Rotation Measure (RM) observations.
- A random vector potential is constructed, obeying a power-law distribution in momentum space,

$$\langle |A_k|^2 \rangle \propto k^{-n} \,,$$

  where $n = 17/3$ corresponds to a turbulent Kolmogorov spectrum.
- The magnetic field is generated using $\tilde{B}_k = ik \times \tilde{A}_k$ and then Fourier-transforming back to position space.
- Note that the power spectrum, $P(k) \sim 2\pi k^2 |B_k|^2 \propto k^{-n+4}$ (so eg. for $n = 17/3$, $P(k) \propto k^{-5/3}$).
- This results in a multi-scale, tangled, divergence-free field with Gaussian statistics.

# Magnetic field model: general properties

- The ICM density in the central region of Coma is well-described by a "$\beta$-model",

$$n_e(r) = n_0 \left(1 + \frac{r^2}{r_c^2}\right)^{-\frac{3}{2}\beta} .$$

- Here $n_0$ is the central electron density and $r_c$ is the core radius.
- Observations: $n_0 = 3.44 \times 10^{-3}\,\mathrm{cm}^{-3}$; $r_c = 291\,\mathrm{kpc}$; $\beta = 0.75$.
- Assume the magnitude of the magnetic field follows a related distribution,

$$B(r) = B_0 \left(\frac{n_e(r)}{n_0}\right)^{\eta} ,$$

  where $\eta$ is another parameter of our model.
- $B_0$ is the average magnitude of the magnetic field over some core region, hence varying $\eta$ will change $B_0$ for any given model.

# Numerical implementation

- We generated a numerical model of the Coma magnetic field using C++, for a $2000^3$ lattice with cell size $s = 0.5\,\text{kpc}$.
- To make the computation tractable, we restrict to components with

$$k_{\text{min}} \leq k \leq k_{\text{max}} \,.$$

  This results in a magnetic field with structure on scales greater than $\Lambda_{\text{max}} = 2\pi/k_{\text{min}}$ and smaller than $\Lambda_{\text{min}} = 2\pi/k_{\text{max}}$.
- Note that there is an effective degeneracy between $\Lambda_{\text{max}}$ and $n$ (the power spectrum index), since both encode information about the scales at which power is concentrated.
- Next we need to propagate axions through this field.

# Numerical implementation

- The axion-photon system evolves iteratively as

$$\begin{pmatrix} |\gamma_\perp\rangle \\ |\gamma_\parallel\rangle \\ |a\rangle \end{pmatrix}_{n+1} = \exp\left(-iL\begin{pmatrix} \Delta_{\gamma,n}+\omega & 0 & \Delta_{\gamma ax,n} \\ 0 & \Delta_{\gamma,n}+\omega & \Delta_{\gamma ay,n} \\ \Delta_{\gamma ax,n} & \Delta_{\gamma ay,n} & \Delta_{a,n}+\omega \end{pmatrix}\right)\begin{pmatrix} |\gamma_\perp\rangle \\ |\gamma_\parallel\rangle \\ |a\rangle \end{pmatrix}_{n}.$$

- Axions convert only into the photon component parallel to the magnetic field direction, so for each cell:
  - the 3-body system is rotated to align with the magnetic field ($U_1$);
  - the 2-body axion-photon mixing state is diagonalised ($U_2$).
- Propagation across the whole of Coma is then described by

$$|\text{final}\rangle = \prod_n U_{1,n}^T U_{2,n}^T \mathcal{M}_n U_{2,n} U_{1,n} |\text{initial}\rangle ,$$

where $\mathcal{M}_n$ is the fully diagonalised propagation matrix.

# Results

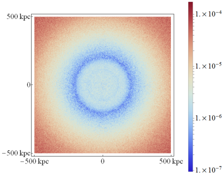


**(a)** 25 eV

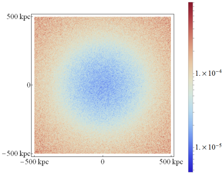


**(b)** 50 eV

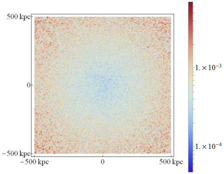


**(c)** 150 eV

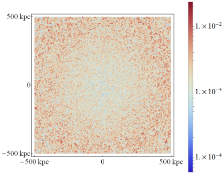


**(d)** 300 eV

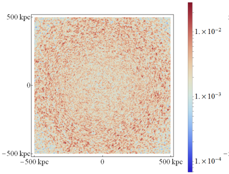


**(e)** 400 eV

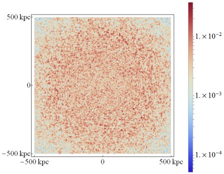


**(f)** 600 eV

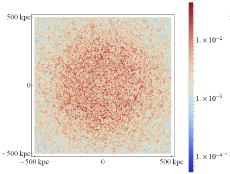


**(g)** 1000 eV

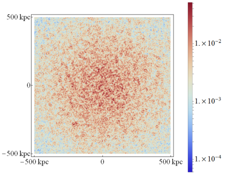


**(h)** 2000 eV

**Figure:** Conversion probabilities for various axion energies, with $\eta = 0.5$, $B_0 = 4.7\,\mu\mathrm{G}$, $\Lambda_{\mathrm{min}} = 2\,\mathrm{kpc}$, $\Lambda_{\mathrm{max}} = 34\,\mathrm{kpc}$, $n = 17/3$ and $M = 5 \cdot 10^{12}\,\mathrm{GeV}$.

# Results

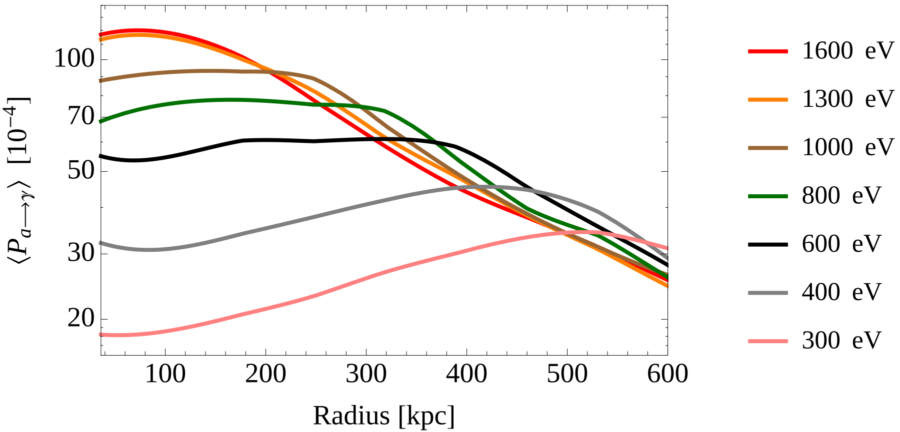


**Figure:** Conversion probabilities as a function of radius, with $\eta = 0.5$, $B_0 = 4.7\,\mu$G, $\Lambda_{min} = 2$ kpc, $\Lambda_{max} = 34$ kpc, $n = 17/3$ and $M = 5 \cdot 10^{12}$ GeV.

# Results: general features

In all our simulations of the soft excess, we found the following:

- The overall conversion probabilities increase with axion energy $\omega$, up to a maximum value where they saturate.
- For lower energies, conversion is suppressed in the cluster centre.
- Conversion increases with radius until it saturates at $r_{\max}(\omega)$; above this radius the probabilities follow a common attenuation curve, independent of $\omega$.
- The radius $r_{\max}(\omega)$ is a decreasing function of $\omega$.
- Increasing $\eta$ enhances conversion in the centre and suppresses it at larger radii (expected, since $B(r)$ attenuates faster for larger $\eta$).
- At very low energies, $\lesssim 50\,\text{eV}$, hints of oscillatory behaviour (recall that $P(a \to \gamma) \simeq \theta^2 \sin^2(\Delta)$, where $\Delta \sim n_e(r)L/\omega$).

# Results for Coma — models considered

We compare the luminosity at given radii with data presented in a 38-cluster survey (Bonamente et al., 2002).

- **Model 1:** Baseline model. Uses parameters $\Lambda_{\rm min} = 2\,$kpc, $\Lambda_{\rm max} = 34\,$kpc, $n = 17/3$, $\eta = 0.4 - 0.7$ and $B_0 = 3.9 - 5.4\,\mu$G.
- **Model 2:** Decrease $\Lambda_{\rm max}$ to 5 kpc, which concentrates power on smaller scales. In addition, use $\eta = 0.7$ and $B_0 = 5.4\,\mu$G.
- **Model 3:** Flat power spectrum ($n = 4$). To fit RM data we need to compensate by increasing $\Lambda_{\rm max}$ to 100 kpc. $\eta = 0.7$; $B_0 = 5.4\,\mu$G.

The results are normalised such that $\Delta N_{\rm eff} = 0.5$ and the total luminosity in the "C-band" ($200 - 400\,$eV) within 500 kpc equals the total observed luminosity quoted by Bonamente et al. (2002),

$$\mathcal{L}_{\rm total} = 1.31 \cdot 10^{43}\,{\rm erg\,s^{-1}}\,.$$

This allows us to predict the axion-photon coupling $M$ for each model.

# Model comparison

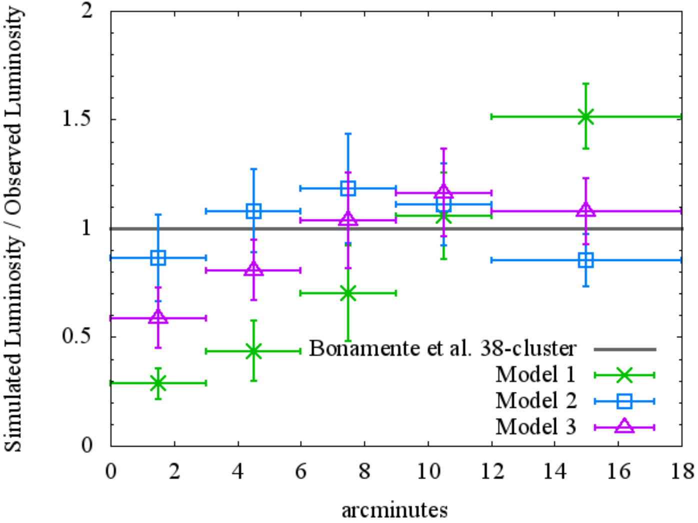

# Prediction for M

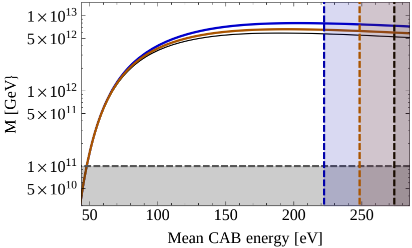


**(a)** ‘Thermal soft excess.’

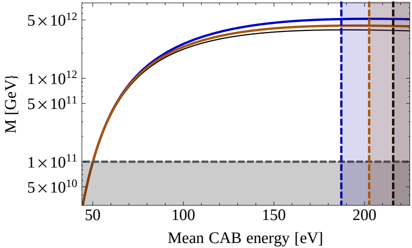


**(b)** ‘Non-thermal soft excess.’

**Figure:** Predicted $M$ vs. mean axion energy. Key: Model 1; Model 2; Model 3.

- For each model we predicted the inverse axion-photon coupling $M$, for both thermal and power-law fits to the soft excess.
- Lower regions excluded by supernova cooling; right-hand regions excluded by limits on X-ray emission at energies $\gtrsim 0.5\,\text{keV}$.
- Global upper bound: $M \lesssim 10^{13}\,\text{GeV}$.

# Summary II

- The soft X-ray excess from galaxy clusters is a long-standing astrophysical puzzle.
- For the Coma cluster, we computed the morphology of the soft X-ray spectrum produced by a Cosmic Axion Background.
- This matches observations, provided the magnetic field has sufficient power on small scales, for an inverse axion-photon coupling

$$10^{11}\,\mathrm{GeV} \lesssim M \lesssim 10^{13}\,\mathrm{GeV}$$

and a mean CAB energy

$$50\,\mathrm{eV} \lesssim \langle \omega_{\mathrm{CAB}} \rangle \lesssim 250\,\mathrm{eV}\,.$$

# Outlook

Possible future directions for my work:

- Other string models: compute DR production in other string-inspired scenarios, compare with $\Delta N_{\mathrm{eff}}$ limits.
- Consistent scenarios: explore other aspects of string phenomenology (inflation, baryogenesis, ...) and try to build models that satisfy multiple constraints simultaneously.
- Magnetic field model: test against a more realistic B-field from a magnetohydrodynamic (MHD) simulation of cluster formation.
- 3.5 keV line: investigate scenarios that (may) fit current observations (e.g. DM$\rightarrow a \rightarrow \gamma$) and build phenomenological models that realise them.